The Heteronuclear Cluster Chemistry of the Group 1B Metals. Part 10.[1] Synthesis, Structures, and Dynamic Behaviour of the Bimetallic Hexanuclear Group 1B Metal Cluster Compounds $[M_2Ru_4(\mu_3\text{-}H)_2\{\mu\text{-}Ph_2As(CH_2)_nEPh_2\}(CO)_{12}]$ (M = Cu or Ag; E = As or P; n = 1 or 2). *X*-Ray Crystal Structure of $[Cu_2Ru_4(\mu_3\text{-}H)_2\{\mu\text{-}Ph_2As(CH_2)_2PPh_2\}(CO)_{12}]$†

Scott S. D. Brown, Paul J. McCarthy, and Ian D. Salter*
Department of Chemistry, University of Exeter, Exeter EX4 4QD
Paul A. Bates and Michael B. Hursthouse
Department of Chemistry, Queen Mary College, University of London, London E1 4NS
Ian J. Colquhoun and William McFarlane
Department of Chemistry, City of London Polytechnic, London EC3N 2EY
Martin Murray
Department of Organic Chemistry, University of Bristol, Bristol BS8 1TS

Treatment of a dichloromethane solution of the salt $[N(PPh_3)_2]_2[Ru_4(\mu\text{-}H)_2(CO)_{12}]$ with two equivalents of the complex $[M(NCMe)_4]PF_6$ (M = Cu or Ag) at −30 °C, followed by the addition of one equivalent of the appropriate bidentate ligand $Ph_2As(CH_2)_nEPh_2$ (E = As or P; n = 1 or 2) affords the mixed-metal cluster compounds $[M_2Ru_4(\mu_3\text{-}H)_2\{\mu\text{-}Ph_2As(CH_2)_nEPh_2\}(CO)_{12}]$ [M = Cu, E = P, n = 1 (**1**) or 2 (**2**); M = Ag, E = P, n = 1 (**3**) or 2 (**4**); M = Cu, E = As, n = 1 (**5**) or 2 (**6**); M = Ag, E = As, n = 1 (**7**) or 2 (**8**)] in *ca.* 60—75% yield. A single-crystal *X*-ray diffraction study on (**2**) reveals that the metal skeleton consists of a tetrahedron of ruthenium atoms capped by a Cu atom [Group 1B metal site M(2)], with one of the $CuRu_2$ faces of the $CuRu_3$ tetrahedron so formed further capped by the second Cu atom [Group 1B metal site M(1)] to give a capped trigonal-bipyramidal metal core geometry. The other two $CuRu_2$ faces of the cluster are both capped by triply bridging hydrido ligands, each ruthenium atom carries three terminal CO groups, and the $Ph_2As(CH_2)_2PPh_2$ ligand bridges the Cu–Cu vector. Disorder between As and P atoms suggests that two distinct structural isomers, the major one with the As atom attached to Cu(2) and the minor one with the As atom bonded to Cu(1), exist in the solid state. Spectroscopic data imply that (**1**) and (**3**)—(**8**) all adopt similar metal framework structures to (**2**). Variable-temperature ^1H and $^{31}P\text{-}\{^1H\}$ n.m.r. studies demonstrate that two structural isomers exist in solution at low temperatures for both copper–ruthenium clusters (**1**) and (**2**) and that each of these pairs of isomers undergoes interconversion at ambient temperature by a dynamic process involving an intramolecular metal core rearrangement. The silver–ruthenium clusters (**3**) and (**4**) undergo similar dynamic behaviour at −30 °C, but no spectra consistent with the ground-state structures could be obtained at lower temperatures. At higher temperatures, (**3**) and (**4**) both undergo two additional dynamic processes. The first involves a novel intramolecular exchange of the arsenic and phosphorus atoms in the $Ph_2As(CH_2)_nPPh_2$ ligands between the two silver atoms in each cluster and, as the temperature is raised further, the bidentate ligands undergo intermolecular exchange between clusters. N.m.r. spectroscopic data suggest that (**6**)—(**8**), which contain $Ph_2As(CH_2)_nAsPh_2$ ligands, also undergo fluxional processes involving Group 1B metal site-exchange at ambient temperature in solution and this behaviour has been directly observed for (**7**) by $^{109}Ag\text{-}\{^1H\}$ INEPT n.m.r. spectroscopy.

Although a large number of mixed-metal cluster compounds containing $M(PR_3)$ (M = Cu, Ag, or Au; R = alkyl or aryl) units have now been reported,[2] similar species in which bidentate ligands are attached to the coinage metals remain relatively rare.[1,3–7] We have previously described[1,6] a series of clusters $[M_2Ru_4(\mu_3\text{-}H)_2\{\mu\text{-}Ph_2P(CH_2)_nPPh_2\}(CO)_{12}]$ (M = Cu or Ag; n = 1—6), in which the bidentate diphosphine ligands bridge the two coinage metals. Although these clusters all adopt capped trigonal-bipyramidal metal framework structures, with the two coinage metals occupying inequivalent sites, multinuclear n.m.r. studies show that the metal skeletons are stereochemically non-rigid in solution at ambient temperature and that dynamic behaviour involving coinage metal site-exchange occurs.[1,6] In view of these novel properties, we have extended this work to the synthesis of analogous clusters in which the coinage metals are linked together by the bidentate ligands $Ph_2As(CH_2)_nEPh_2$ (E = As or P; n = 1 or 2). We wished to investigate the effect of these ligands on the skeletal geometries and dynamic behaviour of the clusters and our interest in preparing species containing the asymmetrical ligands $Ph_2As(CH_2)_nPPh_2$ was also stimulated by the possibility of structural isomerism occurring. Two different

† 3,3,3,4,4,4,5,5,5,6,6,6-Dodecacarbonyl-1,2-μ-[1′-(diphenylarsino)-2′-(diphenylphosphino)ethane-*As*(Cu^1)*P*(Cu^2)(major isomer); *P*(Cu^1)*As*-(Cu^2)(minor isomer)]-1,3,5;1,4,5-di-μ_3-hydrido-*cyclo*-dicoppertetraruthenium(*Cu–Cu*, 5 *Cu–Ru*, 6 *Ru–Ru*).

Supplementary data available: see Instructions for Authors, *J. Chem. Soc., Dalton Trans.*, 1988, Issue 1, pp. xvii—xx.

structural isomers (labelled **A** and **B** in Figure 1) are possible, as either an arsenic atom or a phosphorus atom can be attached to each of the two distinct coinage metal sites. A preliminary account describing some of our results has already been published.[8]

Results and Discussion

Treatment of a dichloromethane solution of the salt $[N(PPh_3)_2]_2[Ru_4(\mu\text{-}H)_2(CO)_{12}]$[9] with two equivalents of the complex $[M(NCMe)_4]PF_6$ (M = Cu or Ag) at −30 °C, followed by the addition of one equivalent of the appropriate bidentate ligand $Ph_2As(CH_2)_nEPh_2$ affords the dark red cluster compounds $[M_2Ru_4(\mu_3\text{-}H)_2\{\mu\text{-}Ph_2As(CH_2)_nEPh_2\}(CO)_{12}]$ [M = Cu, E = P, *n* = 1 (**1**) or 2 (**2**); M = Ag, E = P, *n* = 1 (**3**) or 2 (**4**); M = Cu, E = As, *n* = 1 (**5**) or 2 (**6**); M = Ag, E = As, *n* = 1 (**7**) or 2 (**8**)] in *ca.* 60—75% yield. The clusters (**1**)—(**8**) were characterized by microanalysis and by spectroscopic measurements (Tables 1 and 2). The i.r. spectra of (**1**)—(**8**) are almost identical and they are closely similar to those previously reported[1,6,10] for the clusters $[M_2Ru_4(\mu_3\text{-}H)_2(CO)_{12}L_2]$ [M = Cu, L = PPh_3 or L_2 = μ-$Ph_2P(CH_2)_n$-PPh_2, *n* = 2, 3, or 5; M = Ag, L = PPh_3 or L_2 = μ-Ph_2PCH_2-PPh_2], implying that (**1**)—(**8**) all adopt the same capped trigonal-bipyramidal metal core structure as that established by single-crystal *X*-ray diffraction studies for the latter species. However, to confirm the conclusions drawn from the spectroscopic data, a single-crystal *X*-ray diffraction study was performed on $[Cu_2Ru_4(\mu_3\text{-}H)_2\{\mu\text{-}Ph_2As(CH_2)_2PPh_2\}(CO)_{12}]$ (**2**). Discussion of the variable-temperature n.m.r. data is deferred until the *X*-ray diffraction results have been presented.

The molecular structure of (**2**) is shown in Figure 2, which also shows the crystallographic numbering. Like its Ph_2P-$(CH_2)_2PPh_2$-containing analogue,[6] compound (**2**) crystallizes with two independent molecules (1 and 2) in the asymmetric unit. Selected interatomic distances and angles for both molecules of (**2**) are summarized in Table 3.

The metal skeleton of (**2**) adopts the expected capped trigonal-bipyramidal structure. The four Ru atoms form a tetrahedron,

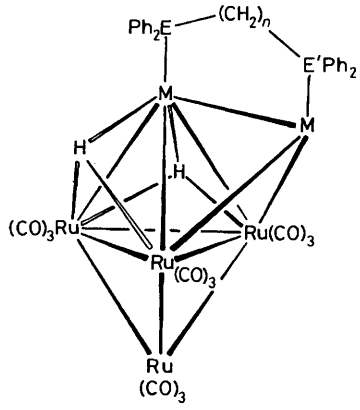

	M	E	E′	*n*
(**1**)	Cu	As or P	P or As	1
(**2**)	Cu	As or P	P or As	2
(**3**)	Ag	As or P	P or As	1
(**4**)	Ag	As or P	P or As	2
(**5**)	Cu	As	As	1
(**6**)	Cu	As	As	2
(**7**)	Ag	As	As	1
(**8**)	Ag	As	As	2

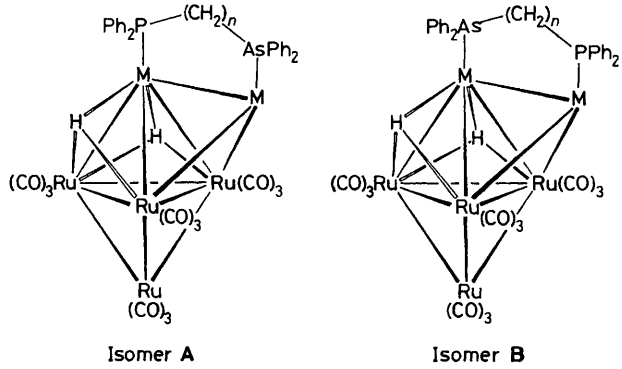

Figure 1. The two possible structural isomers of $[M_2Ru_4(\mu_3\text{-}H)_2\{\mu\text{-}Ph_2As(CH_2)_nPPh_2\}(CO)_{12}]$ [M = Cu, *n* = 1 (**1**) or 2 (**2**); M = Ag, *n* = 1 (**3**) or 2 (**4**)]

Table 1. Analytical[a] and physical data for the heteronuclear clusters $[M_2Ru_4(\mu_3\text{-}H)_2\{\mu\text{-}Ph_2As(CH_2)_nEPh_2\}(CO)_{12}]$ (M = Cu or Ag; E = As or P; *n* = 1 or 2)

Compound	M.p. (decomp.)/°C	$\nu_{max.}$(CO)[b]/cm^{-1}	Yield (%)[c]	Analysis C	Analysis H
(**1**) $[Cu_2Ru_4(\mu_3\text{-}H)_2(\mu\text{-}Ph_2AsCH_2PPh_2)(CO)_{12}]$	142—146	2 068s, 2 032vs, 2 017vs, 2 007s, 1 982 (sh), 1 974m, br, and 1 927w, br	75	34.1 (34.2)	1.8 (1.9)
(**2**) $[Cu_2Ru_4(\mu_3\text{-}H)_2\{\mu\text{-}Ph_2As(CH_2)_2PPh_2\}(CO)_{12}]$	142—144	2 069s, 2 032vs, 2 018vs, 2 005s, 1 984 (sh), 1 975m, br, and 1 930w,br	72	34.9 (34.8)	2.0 (2.0)
(**3**) $[Ag_2Ru_4(\mu_3\text{-}H)_2(\mu\text{-}Ph_2AsCH_2PPh_2)(CO)_{12}]$	134—137	2 067s, 2 030vs, 2 015vs, 2 004s, 1 977 (sh), 1 969m, br, and 1 929w, br	68	32.2 (32.1)	1.8 (1.8)
(**4**) $[Ag_2Ru_4(\mu_3\text{-}H)_2\{\mu\text{-}Ph_2As(CH_2)_2PPh_2\}(CO)_{12}]$	143—146	2 067s, 2 030vs, 2 016vs, 2 002s, 1 979 (sh), 1 969m, br, and 1 929w, br	65	32.8 (32.6)	2.0 (1.9)
(**5**) $[Cu_2Ru_4(\mu_3\text{-}H)_2(\mu\text{-}Ph_2AsCH_2AsPh_2)(CO)_{12}]$	122—124	2 072s, 2 036vs, 2 022vs, 2 010s, 1 979m, br, and 1 934w, br	61	33.3 (33.1)	2.0 (1.8)
(**6**) $[Cu_2Ru_4(\mu_3\text{-}H)_2\{\mu\text{-}Ph_2As(CH_2)_2AsPh_2\}(CO)_{12}]$	124—128	2 072s, 2 035vs, 2 022vs, 2 008s, 1 978m, br, and 1 933w, br	65	33.8 (33.7)	1.9 (1.9)
(**7**) $[Ag_2Ru_4(\mu_3\text{-}H)_2(\mu\text{-}Ph_2AsCH_2AsPh_2)(CO)_{12}]$	144—147	2 071s, 2 035vs, 2 020vs, 2 007s, 1 976m, br, and 1 936w, br	74	31.2 (31.1)	1.8 (1.7)
(**8**) $[Ag_2Ru_4(\mu_3\text{-}H)_2\{\mu\text{-}Ph_2As(CH_2)_2AsPh_2\}(CO)_{12}]$	152—156	2 070s, 2 033vs, 2 019vs, 2 005s, 1 974m, br, and 1 933w, br	69	31.7 (31.6)	2.0 (1.8)

[a] Calculated values given in parentheses. [b] Measured in dichloromethane solution. [c] Based on ruthenium reactant.

Table 2. N.m.r. data[a] for the new Group 1B metal heteronuclear cluster compounds

Compound	^{1}H Data[b]	Low-temperature ^{1}H hydrido ligand signal[b,c]	^{31}P-{^{1}H} Data[d]	Low-temperature ^{31}P-{^{1}H} data[c,d]
(1)	−18.05 [d, 2 H, μ_3-H, J(PH) 8], 3.24 [d, 2 H, $AsCH_2P$, J(PH) 10], 7.05—7.55 (m, 20 H, Ph)	−17.88 [d, 1.0 H, Isomer **A**, J(PH) 12], −18.14 (s, 0.16 H, Isomer **B**)	−1.4 (s,br)	3.8(s, 1.0 P, CH_2PCu, Isomer **A**), −8.1 (s, 0.16 P, CH_2PCu, Isomer **B**)
(2)	−17.76 [d, 2 H, μ_3-H, J(PH) 3], 2.48—2.64 [m, 4 H, $As(CH_2)_2P$], 7.37—7.59 (m, 20 H, Ph)	[e] −17.81 (s, 1.0 H, Isomer **B**), −17.87 [d, 0.37 H, Isomer **A**, J(PH) 13]	−2.6 (s, br)	3.6 [s, 0.37 P, $(CH_2)_2PCu$, Isomer **A**], −5.1 [s, 1.0 P, $(CH_2)_2PCu$, Isomer **B**]
(3)	[f] −17.85 [m, 2 H, μ_3-H, $J(^{109}Ag_pH)$ 35.3, $J(^{107}Ag_pH)$ 30.7, J(PH) 9.2, $J(Ag_{As}H)_{av.}$ 4.5], 3.31 [d of d, 2 H, $AsCH_2P$, J(PH) 9, $J(AgH)_{av.}$ 4], 7.20—7.46 (m, 20 H, Ph)	−17.91 [d of d, br, 2 H, $J(AgH)_{av.}$ 34, J(PH) 10]	[g] 10.3 [2 × d of d, $J(^{109}AgP)$ 570, $J(^{107}AgP)$ 494, $^2J(AgP)_{av.}$ 9]	11.0 [2 × d, br, $J(^{109}AgP)$ 585, $J(^{107}AgP)$ 514]
[h](4)	[i] −17.56 [m, 2 H, μ_3-H, $J(^{109}Ag_pH)$ 22.3, $J(^{107}Ag_pH)$ 19.4, $J(^{109}Ag_{As}H)$ 16.4, $J(^{107}Ag_{As}H)$ 14.3, J(PH) 5.7], 2.26—2.49 [m, 4 H, $As(CH_2)_2P$], 7.02—7.72 (m, 20 H, Ph)	−17.56 to −17.67 (m, br, 2 H)	[g] 11.9 [2 × d of d, $J(^{109}AgP)$ 529, $J(^{107}AgP)$ 459, $^2J(AgP)_{av.}$ 8]	[i] *ca.* 12 [d, vbr, $J(AgP)_{av.}$ *ca.* 490]
[j](5)	−17.88 (s, 2 H, μ_3-H), 3.23 (s, 2 H, $AsCH_2As$), 7.34—7.48 (m, 20 H, Ph)	−18.00 (s, br)		
[k](6)	−17.68 (s, 2 H, μ_3-H), 2.68 [s, 4 H, $As(CH_2)_2As$], 7.42—7.56 (m, 20 H, Ph)	[l] −17.79 (s, br)		
[m](7)	−17.66 [t, 2 H, μ_3-H, $J(AgH)_{av.}$ 19], 3.23 (s, 2 H, $AsCH_2As$), 7.14—7.62 (m, 20 H, Ph)	−17.88 [t, br, 2 H, $J(AgH)_{av.}$ 20]		
(8)	−17.53 [t, 2 H, μ_3-H, $J(AgH)_{av.}$ 19], 2.58 [s, 4 H, $As(CH_2)_2As$], 7.45—7.55 (m, 20 H, Ph)	[e] −17.59 [t, br, 2 H, $J(AgH)_{av.}$ 20]		

[a] Chemical shifts (δ) in p.p.m., coupling constants in Hz, measured at ambient temperature, unless otherwise stated. [b] Measured in [$^2H_2$]dichloromethane solution. [c] Measured at −90 °C, unless otherwise stated. [d] Hydrogen-1 decoupled, measured in [$^2H_2$]dichloromethane–CH_2Cl_2 solution; chemical shifts positive to high frequency of 85% H_3PO_4 (external). [e] Measured at −80 °C. [f] Measured at −40 °C. [g] Measured at −30 °C. [h] High-field hydrido ligand signal at 25 °C, δ −17.48 [apparent d of t of t, 2 H, $J(^{109}AgH)$ 19.4, $J(^{107}AgH)$ 16.9, J(PH) 5.7 Hz]. [i] Measured at −70 °C. [j] ^{13}C-{^{1}H} data (CD_2Cl_2–CH_2Cl_2): δ 197.9 (CO), 133.2 [C^1(Ph)], 132.5 [C^2(Ph)], 130.9 [C^4(Ph)], 129.6 [C^3(Ph)], and 25.0 (CH_2). Carbonyl region at −100 °C, δ 200.6 (s, br, CO), 198.1 (s, br, CO), 196.8 (s, br, CO), 195.3 (s, br CO), and 193.1 (s br, CO). [k] ^{13}C-{^{1}H} data (CD_2Cl_2–CH_2Cl_2): δ 197.8 (CO), 132.6 [C^2(Ph)], 132.1 [C^4(Ph)], 131.0 [C^1(Ph)], 129.8 [C^3(Ph)], and 22.7 (CH_2). Carbonyl and methylene region at −100 °C, δ 200.1 (s, 2 CO), 198.5 (s, 2 CO), 197.7 (s, 1 CO), 196.9 (s, 2 CO), 196.7 (s, 2 CO), 195.1 (s, 2 CO), 192.8 (s, 1 CO), 21.5 (s, 1 C, CH_2), and 21.1 (s, 1 C, CH_2). [l] Measured at −100 °C. [m] ^{109}Ag-{^{1}H} INEPT data (CH_2Cl_2–C_6D_6): $^{107}Ag^{109}Ag$ isotopomer, δ −800 p.p.m. [d, $J(^{107}Ag^{109}Ag)$ 40 Hz]; $^{109}Ag^{109}Ag$ isotopomer, δ −800 p.p.m. Chemical shifts are positive to high frequency of external $[Ag\{P(OEt)_3\}_4]NO_3$.

with one face [Ru(11)Ru(13)Ru(14)] capped by a copper atom [Cu(12)], and the Cu(12)Ru(13)Ru(14) face of the $CuRu_3$ tetrahedron so formed is further capped by a second copper atom [Cu(11)]. Both the Cu(12)Ru(11)Ru(13) and the Cu(12)Ru(11)Ru(14) faces of the metal framework are capped by a triply bridging hydrido ligand, the Ru atoms are all ligated by three terminal CO groups, which are essentially linear, and the $Ph_2As(CH_2)_2PPh_2$ ligand bridges the Cu–Cu vector. The variations in length between the equivalent metal–metal separations in molecules 1 and 2 of (**2**) are similar to those observed for its $Ph_2P(CH_2)_2PPh_2$-containing analogue[6] and the mean distances of the equivalent metal–metal contacts in the two clusters vary very little. The two independent molecules were refined with the arsenic atom of the asymmetrical bidentate ligand attached to copper site Cu(2) and the phosphorus atom bonded to copper site Cu(1). However, the As and P thermal parameters and the Cu–E (E = As or P) bond lengths strongly suggest some mixing of the As and P atoms, probably by different amounts for molecules 1 and 2 (see Experimental section). Thus, it seems that both of the possible structural isomers (**A** and **B** in Figure 1) of (**2**) exist in the solid state, but that the major isomer present is **B**.

At −90 °C, the ^{31}P-{^{1}H} n.m.r. spectra of the copper-containing clusters (**1**) and (**2**) both show two signals with different intensities [relative intensities (r.i.) 1.0:0.16 and 0.37:1.0, respectively]. Thus, for (**1**) and (**2**), both of the two possible structural isomers (**A** and **B** in Figure 1) are present in solution at low temperature. In each case, the two ^{31}P-{^{1}H} n.m.r. peaks broaden and eventually coalesce into a singlet as the temperature is raised. The observation of these averaged phosphorus environments demonstrates that some dynamic process is interconverting the two distinct structural isomers of each cluster at ambient temperature in solution. It is reasonable to propose that the dynamic behaviour exhibited by (**1**) and (**2**) involves an intramolecular metal core rearrangement, as we have previously shown[1,6,10] that the structurally very closely related species $[M_2Ru_4(\mu_3\text{-}H)_2(CO)_{12}L_2]$ [M = Cu or Ag, L = PPh_3 or L_2 = μ-$Ph_2P(CH_2)_nPPh_2$, n = 1—6] all undergo a fluxional process which exchanges the coinage metals between the two distinct sites in their capped trigonal-bipyramidal metal skeletons.

The conclusions drawn from the ^{31}P-{^{1}H} n.m.r. data are confirmed by variable-temperature ^{1}H n.m.r. studies on the high-field hydrido ligand signals of (**1**) and (**2**), which also show

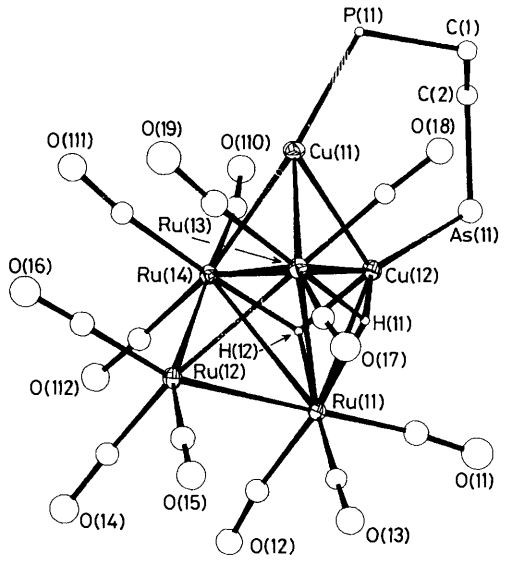

Figure 2. Molecular structure of $[Cu_2Ru_4(\mu_3\text{-}H)_2\{\mu\text{-}Ph_2As(CH_2)_2PPh_2\}(CO)_{12}]$ (**2**), molecule 1, showing the crystallographic numbering. For molecule 2, the first digit of each number is changed from 1 to 2, except for C(1) and C(2) in molecule 1, which are equivalent to C(3) and C(4), respectively. The phenyl groups have been omitted for clarity and the carbon atom of each carbonyl group has the same number as the oxygen atom

the presence of two distinct structural isomers for each cluster at low temperatures. At −90 °C, a singlet and a doublet [J(PH) 12 Hz] (r.i. 0.16:1.0) are observed for (**1**) and these two signals broaden and eventually coalesce as the temperature is raised. An averaged signal, consisting of a doublet with a smaller coupling constant [J(PH) 8 Hz], is visible at ambient temperature. From previous work on structurally related species,[2,6,10] isomer **A**, in which the phosphorus is attached to the copper atom bonded to the hydrido ligands, would be expected to show ^{31}P–^{1}H coupling, but isomer **B** would not. Thus, isomer **A** is clearly predominant for (**1**). However, at −80 °C, the hydrido ligand signals for (**2**) consist of a singlet and a doublet [J(PH) 13 Hz] (r.i. 1.0:0.37) (Figure 3). Again these peaks coalesce as the temperature is raised and one doublet, with a much smaller ^{31}P–^{1}H coupling of 3 Hz, is observed at ambient temperature. Therefore, **B** is the major isomer of (**2**) in solution, as well as in the solid state. It is not possible to obtain a quantitative result for the relative proportions of **A** and **B** in the solid state from X-ray diffraction, but the observed mixing of As and P atoms is certainly qualitatively consistent with the observed ratio of **A** and **B** in solution. It is interesting that the formal addition of just one methylene group to the backbone of the asymmetrical bidentate ligand in (**1**) causes such a remarkable change in the relative proportions of **A** and **B**.

The ^{31}P-$\{^{1}H\}$ n.m.r. spectra of the silver clusters (**3**) and (**4**) at −30 °C both show a single phosphorus resonance, which is split into two doublets of doublets by ^{107}Ag–^{31}P and ^{109}Ag–^{31}P couplings through one and two bonds. The spectrum for (**3**) is still sharp at −70 °C, but it begins to broaden at −90 °C. In the case of (**4**), the pattern of signals begins to broaden between −50 and −70 °C, but the cluster is not sufficiently soluble to allow a good quality spectrum to be obtained at −90 °C. Although the ^{31}P-$\{^{1}H\}$ n.m.r. spectra observed at −30 °C are also consistent with (**3**) and (**4**) existing in solution as single isomers with stereochemically rigid metal frameworks, in conjunction with the variable-temperature ^{1}H n.m.r. studies on (**3**) and (**4**) (see below) and the results obtained for the

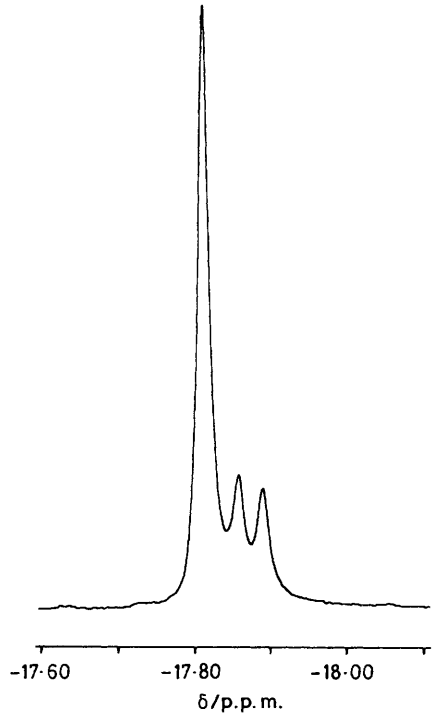

Figure 3. The high-field hydrido ligand signal in the ^{1}H n.m.r. spectrum of $[Cu_2Ru_4(\mu_3\text{-}H)_2\{\mu\text{-}Ph_2As(CH_2)_2PPh_2\}(CO)_{12}]$ (**2**) at −80 °C (CD_2Cl_2). The singlet is due to isomer **B** and the doublet to isomer **A** (r.i. 1.0:0.37)

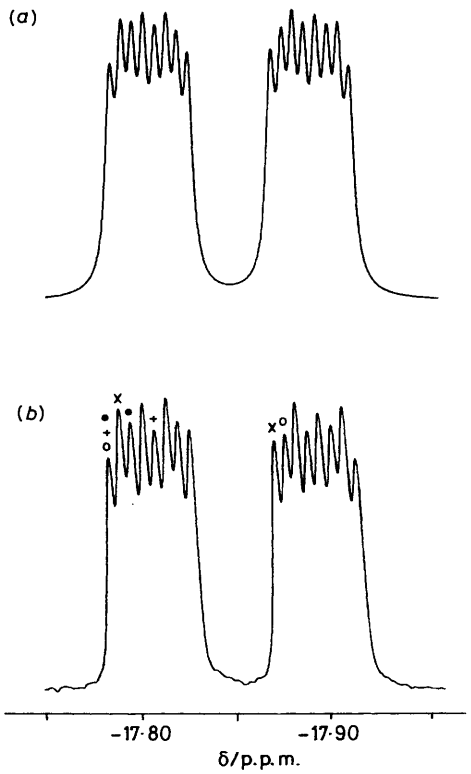

Figure 4. Simulated (*a*) and observed (measured in CD_2Cl_2 solution at −40 °C) (*b*) high-field hydrido ligand signals in the ^{1}H n.m.r. spectrum of $[Ag_2Ru_4(\mu_3\text{-}H)_2(\mu\text{-}Ph_2AsCH_2PPh_2)(CO)_{12}]$ (**3**). Coupling constants are measured in Hz. (○) $J(^{109}Ag_PH)$ 35.3, (×) $J(^{107}Ag_PH)$ 30.7, (+) J(PH) 9.2, (●) $J(Ag_{As}H)_{av.}$ 4.5

Table 3. Selected bond lengths (Å) and angles (°), with estimated standard deviations in parentheses, for $[Cu_2Ru_4(\mu_3\text{-}H)_2\{\mu\text{-}Ph_2As(CH_2)_2PPh_2\}(CO)_{12}]$ (**2**)

(*a*) Molecule 1

Ru(12)–Ru(11)	2.792(6)	Ru(13)–Ru(11)	2.947(6)				
Ru(14)–Ru(11)	2.988(6)	Cu(12)–Ru(11)	2.640(6)				
Ru(13)–Ru(12)	2.789(6)	Ru(14)–Ru(12)	2.791(5)				
Ru(14)–Ru(13)	2.886(6)	Cu(11)–Ru(13)	2.609(6)				
Cu(12)–Ru(13)	2.788(6)	Cu(11)–Ru(14)	2.612(7)				
Cu(12)–Ru(14)	2.687(6)	Cu(12)–Cu(11)	2.494(6)				
P(11)–Cu(11)	2.266(7)	As(11)–Cu(12)	2.249(6)				
C(1C1)–As(11)	1.896(15)	C(1D1)–As(11)	1.846(15)				
C(2)–As(11)	1.933(25)	C(1A1)–P(11)	1.866(15)				
C(1B1)–P(11)	1.844(14)	C(1)–P(11)	1.913(25)				
C(2)–C(1)	1.419(33)						
Ru(13)–Ru(11)–Ru(12)	58.1(2)	Ru(14)–Ru(11)–Ru(12)	57.6(2)				
Ru(14)–Ru(11)–Ru(13)	58.2(2)	Cu(12)–Ru(11)–Ru(12)	105.2(2)				
Cu(12)–Ru(11)–Ru(13)	59.6(2)	Cu(12)–Ru(11)–Ru(14)	56.6(2)				
Ru(13)–Ru(12)–Ru(11)	63.8(2)	Ru(14)–Ru(12)–Ru(11)	64.7(2)				
Ru(14)–Ru(12)–Ru(13)	62.3(2)	Ru(12)–Ru(13)–Ru(11)	58.2(2)				
Ru(14)–Ru(13)–Ru(11)	61.6(2)	Ru(14)–Ru(13)–Ru(12)	58.9(2)				
Cu(11)–Ru(13)–Ru(11)	103.1(2)	Cu(11)–Ru(13)–Ru(12)	112.7(2)				
Cu(11)–Ru(13)–Ru(14)	56.5(2)	Cu(12)–Ru(13)–Ru(11)	54.7(2)				
Cu(12)–Ru(13)–Ru(12)	101.4(2)	Cu(12)–Ru(13)–Ru(14)	56.5(2)				
Cu(12)–Ru(13)–Cu(11)	54.9(2)	Ru(12)–Ru(14)–Ru(11)	57.7(2)				
Ru(13)–Ru(14)–Ru(11)	60.2(2)	Ru(13)–Ru(14)–Ru(12)	58.8(2)				
Cu(11)–Ru(14)–Ru(11)	101.9(2)	Cu(11)–Ru(14)–Ru(12)	112.6(2)				
Cu(11)–Ru(14)–Ru(13)	56.4(2)	Cu(12)–Ru(14)–Ru(11)	55.1(2)				
Cu(12)–Ru(14)–Ru(12)	104.0(2)	Cu(12)–Ru(14)–Ru(13)	59.9(2)				
Cu(12)–Ru(14)–Cu(11)	56.1(2)	Ru(14)–Cu(11)–Ru(13)	67.1(2)				
Cu(12)–Cu(11)–Ru(13)	66.2(2)	Cu(12)–Cu(11)–Ru(14)	63.4(2)				
P(11)–Cu(11)–Ru(13)	136.3(2)	P(11)–Cu(11)–Ru(14)	155.6(2)				
P(11)–Cu(11)–Cu(12)	114.5(3)	Ru(13)–Cu(12)–Ru(11)	65.7(2)				
Ru(14)–Cu(12)–Ru(11)	68.2(2)	Ru(14)–Cu(12)–Ru(13)	63.6(2)				
Cu(11)–Cu(12)–Ru(11)	116.0(2)	Cu(11)–Cu(12)–Ru(13)	58.9(2)				
Cu(11)–Cu(12)–Ru(14)	60.4(2)	As(11)–Cu(12)–Ru(11)	143.1(2)				
As(11)–Cu(12)–Ru(13)	142.5(2)	As(11)–Cu(12)–Ru(14)	137.5(2)				
As(11)–Cu(12)–Cu(11)	100.9(2)	C(1C1)–As(11)–Cu(12)	115.3(7)				
C(1D1)–As(11)–Cu(12)	114.5(6)	C(1D1)–As(11)–C(1C1)	104.3(8)				
C(2)–As(11)–Cu(12)	117.2(8)	C(2)–As(11)–C(1C1)	103.0(10)				
C(2)–As(11)–C(1D1)	100.5(10)	C(1A1)–P(11)–Cu(11)	116.4(7)				
C(1B1)–P(11)–Cu(11)	117.3(6)	C(1B1)–P(11)–C(1A1)	104.5(9)				
C(1)–P(11)–Cu(11)	109.6(8)	C(1)–P(11)–C(1A1)	103.5(10)				
C(1)–P(11)–C(1B1)	103.9(10)	C(2)–C(1)–P(11)	112.5(19)				
C(1)–C(2)–As(11)	117.1(17)	Ru(13)–H(11)–Ru(11)	109.9(3)				
Cu(12)–H(11)–Ru(11)	100.9(3)	Cu(12)–H(11)–Ru(13)	109.1(3)				
Ru(14)–H(12)–Ru(11)	112.2(3)	Cu(12)–H(12)–Ru(11)	100.9(3)				
Cu(12)–H(12)–Ru(14)	103.4(3)						

(*b*) Molecule 2

Ru(22)–Ru(21)	2.792(6)	Ru(23)–Ru(21)	2.959(6)				
Ru(24)–Ru(21)	2.976(6)	Cu(22)–Ru(21)	2.666(6)				
Ru(23)–Ru(22)	2.783(6)	Ru(24)–Ru(22)	2.789(5)				
Ru(24)–Ru(23)	2.894(5)	Cu(21)–Ru(23)	2.655(6)				
Cu(22)–Ru(23)	2.748(6)	Cu(21)–Ru(24)	2.590(6)				
Cu(22)–Ru(24)	2.721(6)	Cu(22)–Cu(21)	2.479(6)				
P(21)–Cu(21)	2.204(8)	As(21)–Cu(22)	2.289(6)				
C(2C1)–As(21)	1.879(14)	C(2D1)–As(21)	1.936(17)				
C(4)–As(21)	1.944(27)	C(2A1)–P(21)	1.849(16)				
C(2B1)–P(21)	1.794(15)	C(3)–P(21)	1.824(26)				
C(4)–C(3)	1.510(36)						
Ru(23)–Ru(21)–Ru(22)	57.8(2)	Ru(24)–Ru(21)–Ru(22)	57.7(2)				
Ru(24)–Ru(21)–Ru(23)	58.4(2)	Cu(22)–Ru(21)–Ru(22)	104.7(2)				
Cu(22)–Ru(21)–Ru(23)	58.2(2)	Cu(22)–Ru(21)–Ru(24)	57.4(2)				
Ru(23)–Ru(22)–Ru(21)	64.1(2)	Ru(24)–Ru(22)–Ru(21)	64.4(2)				
Ru(24)–Ru(22)–Ru(23)	62.6(2)	Ru(22)–Ru(23)–Ru(21)	58.1(2)				
Ru(24)–Ru(23)–Ru(21)	61.1(2)	Ru(24)–Ru(23)–Ru(22)	58.8(2)				
Cu(21)–Ru(23)–Ru(21)	102.1(2)	Cu(21)–Ru(23)–Ru(22)	111.5(2)				
Cu(21)–Ru(23)–Ru(24)	55.4(2)	Cu(22)–Ru(23)–Ru(21)	55.5(2)				
Cu(22)–Ru(23)–Ru(22)	102.8(2)	Cu(22)–Ru(23)–Ru(24)	57.6(2)				
Cu(22)–Ru(23)–Cu(21)	54.6(2)	Ru(22)–Ru(24)–Ru(21)	57.8(2)				
Ru(23)–Ru(24)–Ru(21)	60.5(2)	Ru(23)–Ru(24)–Ru(22)	58.6(2)				
Cu(21)–Ru(24)–Ru(21)	103.3(2)	Cu(21)–Ru(24)–Ru(22)	113.4(2)				
Cu(21)–Ru(24)–Ru(23)	57.6(2)	Cu(22)–Ru(24)–Ru(21)	55.6(2)				
Cu(22)–Ru(24)–Ru(22)	103.3(2)	Cu(22)–Ru(24)–Ru(23)	58.5(2)				
Cu(22)–Ru(24)–Cu(21)	55.6(2)	Ru(24)–Cu(21)–Ru(23)	67.0(2)				
Cu(22)–Cu(21)–Ru(23)	64.6(2)	Cu(22)–Cu(21)–Ru(24)	64.9(2)				
P(21)–Cu(21)–Ru(23)	134.7(2)	P(21)–Cu(21)–Ru(24)	158.3(2)				
P(21)–Cu(21)–Cu(22)	118.9(3)	Ru(23)–Cu(22)–Ru(21)	66.2(2)				
Ru(24)–Cu(22)–Ru(21)	67.1(2)	Ru(24)–Cu(22)–Ru(23)	63.9(2)				
Cu(21)–Cu(22)–Ru(21)	116.3(2)	Cu(21)–Cu(22)–Ru(23)	60.8(2)				
Cu(21)–Cu(22)–Ru(24)	59.5(2)	As(21)–Cu(22)–Ru(21)	146.1(1)				
As(21)–Cu(22)–Ru(23)	138.0(2)	As(21)–Cu(22)–Ru(24)	138.7(1)				
As(21)–Cu(22)–Cu(21)	97.6(2)	C(2C1)–As(21)–Cu(22)	114.0(6)				
C(2D1)–As(21)–Cu(22)	115.6(8)	C(2D1)–As(21)–C(2C1)	103.9(9)				
C(4)–As(21)–Cu(22)	119.1(9)	C(4)–As(21)–C(2C1)	102.5(11)				
C(4)–As(21)–C(2D1)	99.4(11)	C(2A1)–P(21)–Cu(21)	112.8(7)				
C(2B1)–P(21)–Cu(21)	119.9(7)	C(2B1)–P(21)–C(2A1)	106.1(9)				
C(3)–P(21)–Cu(21)	109.4(9)	C(3)–P(21)–C(2A1)	107.6(11)				
C(3)–P(21)–C(2B1)	99.8(10)	C(4)–C(3)–P(21)	115.3(20)				
C(3)–C(4)–As(21)	115.6(18)	Ru(23)–H(21)–Ru(21)	110.6(3)				
Cu(22)–H(21)–Ru(21)	102.3(3)	Cu(22)–H(21)–Ru(23)	106.8(3)				
Ru(24)–H(22)–Ru(21)	111.5(3)	Cu(22)–H(22)–Ru(21)	102.3(3)				
Cu(22)–H(22)–Ru(24)	105.3(3)						

analogous copper clusters (**1**) and (**2**), the broadening of the $^{31}P\text{-}\{^1H\}$ spectra at low temperatures suggests that isomers **A** and **B** are both present in solution for (**3**) and (**4**) and that they are interconverted at −30 °C by a dynamic process involving an intramolecular metal core rearrangement. It would seem that this process has a higher free energy of activation for (**4**), which is consistent with a trend previously reported for the similar intramolecular metal core rearrangements exhibited by $[Ag_2Ru_4(\mu_3\text{-}H)_2\{\mu\text{-}Ph_2P(CH_2)_nPPh_2\}(CO)_{12}]$ (n = 1 or 2).[11]

The variable-temperature ^1H n.m.r. data for (**3**) and (**4**) provide further evidence that the metal skeletons of the clusters undergo rearrangements in solution. Previous studies[6] on analogous species containing $Ph_2P(CH_2)_nPPh_2$ (n = 1—6) ligands demonstrate that, in the ground-state structures, the hydrido ligands only couple with the silver atom bonded to them and to the phosphorus atom attached to that silver atom. The observed values for $J(^{107,109}AgH)_{av.}$ and $J(PH)$ lie in the ranges 25—33 and 9—10 Hz, respectively.[6] Therefore, if the metal skeletons of (**3**) and (**4**) are stereochemically rigid in solution, the high-field ^1H n.m.r. hydrido ligand signals should be split into two doublets by $^{107}Ag\text{–}^1H$ and $^{109}Ag\text{–}^1H$ couplings if the clusters exist as isomer **B**, and each peak of this pattern should be further split into a doublet by $^{31}P\text{–}^1H$ coupling if the clusters adopt the structure of isomer **A**. However, the actual ^1H n.m.r. hydrido ligand signals observed for (**3**) and (**4**) are both more complex than either of the above possibilities. For (**3**), a 16-line pattern, which can be interpreted in terms of a single resonance split into doublets by couplings of 35.3, 30.7, 9.2, and 4.5 Hz, is visible at −40 °C (Figure 4). It is possible to explain this hydrido ligand signal by proposing that isomers **A** and **B** of (**3**) interconvert in solution, with **A** being very much the predominant isomer. If **A** is very much the predominant isomer, then the values of $J(^{109}AgH)$ and $J(^{107}AgH)$ for the silver atom attached to phosphorus [$J(^{109}Ag_PH)$ and $J(^{107}Ag_PH)$] and the value of $J(PH)$ should be very similar to those observed in the ground-state spectra of

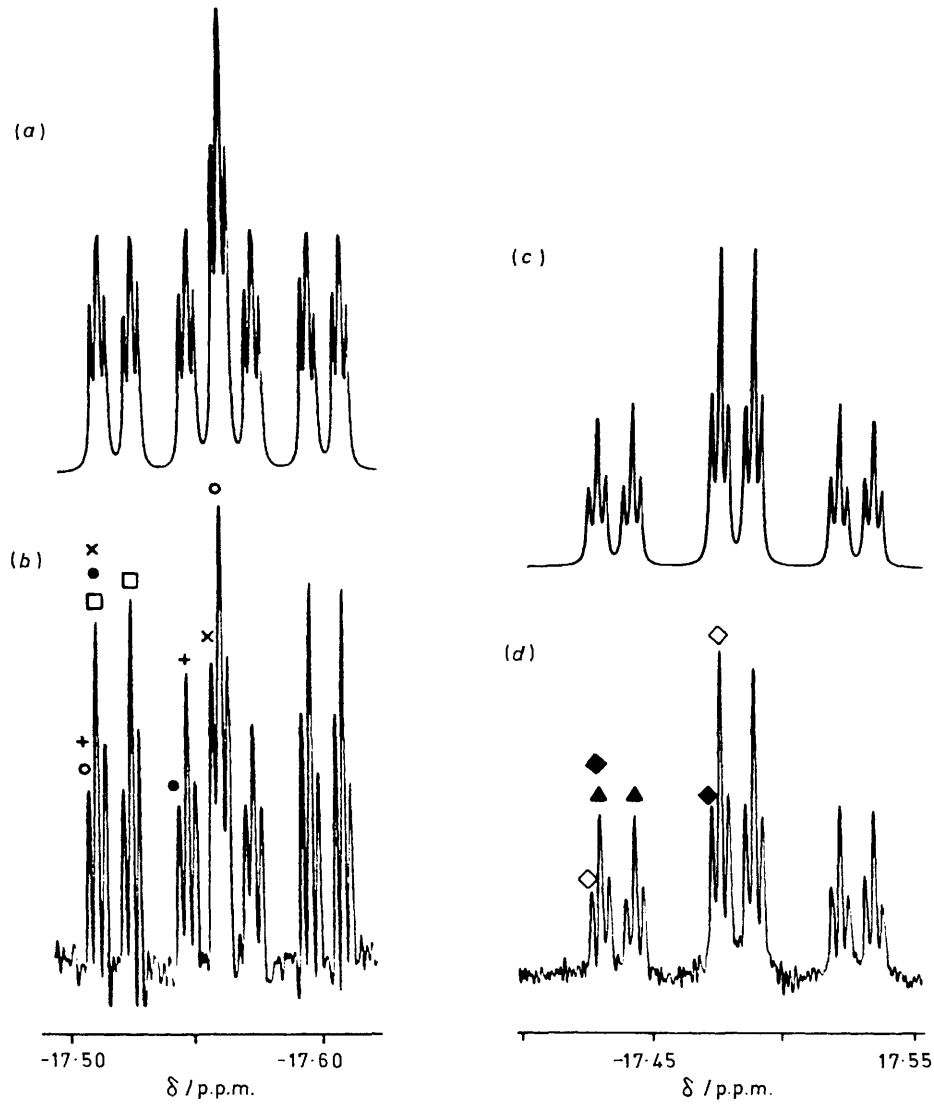

Figure 5. Simulated and observed (measured in CD_2Cl_2 solution) high-field hydrido ligand signals in the ^1H n.m.r. spectrum of $[Ag_2Ru_4(\mu_3\text{-}H)_2\{\mu\text{-}Ph_2As(CH_2)_2PPh_2\}(CO)_{12}]$ (**4**). (*a*) Simulated signal at −30 °C; (*b*) observed signal at −30 °C (Gaussian enhanced); (*c*) simulated signal at 25 °C; (*d*) observed signal at 25 °C. Coupling constants are measured in Hz. For (*a*) and (*b*) (○) $J(^{109}Ag_PH)$ 22.3, (+) $J(^{109}Ag_{As}H)$ 16.4, (×) $J(^{107}Ag_PH)$ 19.4, (●) $J(^{107}Ag_{As}H)$ 14.3, (□) J(PH) 5.7; for (*c*) and (*d*) (◇), $J(^{109}AgH)$ 19.4, (◆) $J(^{107}AgH)$ 16.9, (▲) J(PH) 5.7

the analogous bidentate diphosphine-containing species.[6] Thus, three of the coupling constants in the ^1H n.m.r. hydrido ligand signal of (**3**) at −40 °C can be assigned as follows: $J(^{109}Ag_PH)$ 35.3, $J(^{107}Ag_PH)$ 30.7, and J(PH) 9.2 Hz. The additional coupling of 4.5 Hz is due to the silver atom attached to arsenic $[J(^{107,109}Ag_{As}H)_{av.}]$, with the values of $J(^{109}Ag_{As}H)$ and $J(^{107}Ag_{As}H)$ being too small for the separate contributions from the two silver isotopes to be resolved. The silver atom attached to arsenic will only couple to the hydrido ligands in isomer **B** and, as there is only a small proportion of isomer **B**, the magnitude of $J(^{107,109}Ag_{As}H)_{av.}$ is very much smaller than those of $J(^{109}Ag_PH)$, $J(^{107}Ag_PH)$, and the values of $J(^{109}AgH)$ and $J(^{107}AgH)$ observed for the analogous bidentate diphosphine-containing species.[6] At −100 °C, the hydrido ligand multiplet is slightly broadened, so the $^{107,109}Ag_{As}$–^1H coupling and the separate contributions from $J(^{109}Ag_PH)$ and $J(^{107}Ag_PH)$ can no longer be resolved, but no spectrum consistent with the ground state could be obtained.

The ^1H n.m.r. high-field hydrido ligand signal for (**4**) at −30 °C is a complex multiplet [Figure 5(*b*)] and this pattern of lines can be also explained by postulating that isomers **A** and **B** of the cluster are interconverting in solution. In this case, the values of $J(^{109}Ag_PH)$ and $J(^{107}Ag_PH)$ (22.3 and 19.4 Hz) are much closer to those of $J(^{109}Ag_{As}H)$ and $J(^{107}Ag_{As}H)$ (16.4 and 14.3 Hz) and the value of J(PH) (5.7 Hz) is much lower than that of (**3**). Thus, although **A** is still the predominant isomer for (**4**), the relative proportion of isomer **B** for this cluster is much higher than that of (**3**). As observed for the analogous copper clusters (**1**) and (**2**), the formal addition of one methylene group to the backbone of the asymmetrical bidentate ligand in (**3**) favours isomer **B**, although the change in the relative proportions of the two isomers is not as large for the silver species. At −70 °C, all of the lines in the multiplet hydrido ligand signal of (**4**) are broadened and the central apparent triplet begins to collapse, but unfortunately the cluster is not sufficiently soluble to obtain good quality spectra at lower temperatures.

The ^1H and ^{31}P-$\{^1H\}$ n.m.r. spectra of (**3**) and (**4**) show that,

at higher temperatures, these clusters undergo two more dynamic processes as well as the intramolecular metal core rearrangement. As the temperature is raised from −30 °C, the central apparent triplet of triplets in the multiplet hydrido ligand signal of (**4**) broadens and collapses and, at 25 °C, the total spectrum observed consists of a well-resolved apparent doublet of triplets of triplets [Figure 5(*d*)]. The latter signal is consistent with the hydrido ligands coupling to two equivalent silver atoms and to the phosphorus atom. The dynamic process causing the equivalence of the silver atoms cannot be an intermolecular exchange of $Ph_2As(CH_2)_2PPh_2$ ligands between clusters because the ^{31}P–^{1}H coupling is retained, so we propose that the arsenic and phosphorus atoms of the bidentate ligand undergo novel intramolecular site-exchange between the two silver atoms.* As the temperature is raised further, the hydrido ligand signal again broadens and, at 70 °C, it is a broad triplet. This loss of ^{31}P–^{1}H coupling suggests that the $Ph_2As(CH_2)_2PPh_2$ ligands do undergo intermolecular exchange between clusters at high temperatures. No well-resolved spectra could be obtained at the high-temperature limit, because the cluster decomposed above 70 °C. Some of the lines in the ^{31}P-{^{1}H} n.m.r. spectrum of (**4**) also broaden and collapse as the temperature is raised, which is consistent with the proposed dynamic behaviour, but the cluster is too unstable for any well-resolved high-temperature spectra to be obtained. The ^{1}H n.m.r. hydrido ligand signal and the ^{31}P-{^{1}H} n.m.r. spectra of (**3**) show very similar temperature-dependent behaviour to those of (**4**), although, in this case, no well-resolved apparent doublet of triplets of triplets pattern could be obtained. Thus, it seems very likely that the arsenic and phosphorus atoms of the $Ph_2AsCH_2PPh_2$ ligand in (**3**) also first undergo intramolecular site-exchange between the two silver atoms and then the bidentate ligand undergoes intermolecular exchange between clusters as the temperature is raised from −30 to 60 °C. Again, the cluster proved to be too unstable to allow well-resolved spectra to be obtained at the high-temperature limit.

The dynamic behaviour observed for (**3**) and (**4**) is in marked contrast to that of the analogous clusters $[Ag_2Ru_4(\mu_3\text{-}H)_2\{\mu\text{-}Ph_2P(CH_2)_nPPh_2\}(CO)_{12}]$ (n = 1—6).[1,6] Although all of these species undergo intramolecular metal core rearrangements, the $Ph_2P(CH_2)_nPPh_2$ ligands are not involved in any dynamic processes at ambient temperature in solution. However, intermolecular exchange of monodentate phosphine ligands at room temperature in solution is well established for silver heteronuclear clusters.[4,10,12]

N.m.r. spectroscopic data suggest that the clusters (**6**)—(**8**), which contain $Ph_2As(CH_2)_nAsPh_2$ ligands, also undergo dynamic behaviour involving coinage metal site-exchange at ambient temperature in solution. The ambient-temperature ^{13}C-{^{1}H} n.m.r. spectrum of the copper-containing cluster (**6**) shows a single methylene resonance, whereas the expected two signals are visible at −100 °C. These observations are consistent with an intramolecular metal core rearrangement similar to that exhibited by (**1**)—(**4**) or an intermolecular exchange of $Ph_2As(CH_2)_2AsPh_2$ ligands between clusters. However, as the analogous species which contain $Ph_2E(CH_2)_2PPh_2$ (E = As or P[6]) both undergo the former dynamic process, but not the latter at ambient temperature, it seems likely that the metal skeleton of (**6**) is stereochemically non-rigid in solution also. The high-field hydrido ligand signals in the ambient-temperature ^{1}H n.m.r. spectra of silver-containing species (**7**) and (**8**) are both triplets, with similar values of $J(^{107,109}AgH)$ to those reported for the analogous clusters containing $Ph_2P(CH_2)_nPPh_2$.[6] Thus, although the two silver atoms in (**7**) and (**8**) occupy geometrically distinct sites in the ground-state structures, they are rendered equivalent at ambient temperature in solution. The ^{1}H n.m.r. high-field hydrido ligand signals of (**7**) and (**8**) are also triplets at −90 and −80 °C, respectively, so the metal core rearrangement still operates for the two clusters at these temperatures.

We have very recently reported the results of ^{109}Ag-{^{1}H} INEPT n.m.r. studies on $[Ag_2Ru_4(\mu_3\text{-}H)_2\{\mu\text{-}Ph_2P(CH_2)_nPPh_2\}(CO)_{12}]$ (n = 1, 2, or 4), which provided the first direct evidence that Group 1B metal heteronuclear clusters do undergo intramolecular metal core rearrangements in solution.[1] As (**7**) and (**8**) both show ^{109}Ag–^{1}H coupling, ^{109}Ag-{^{1}H} INEPT n.m.r. spectroscopy can also be used to investigate their

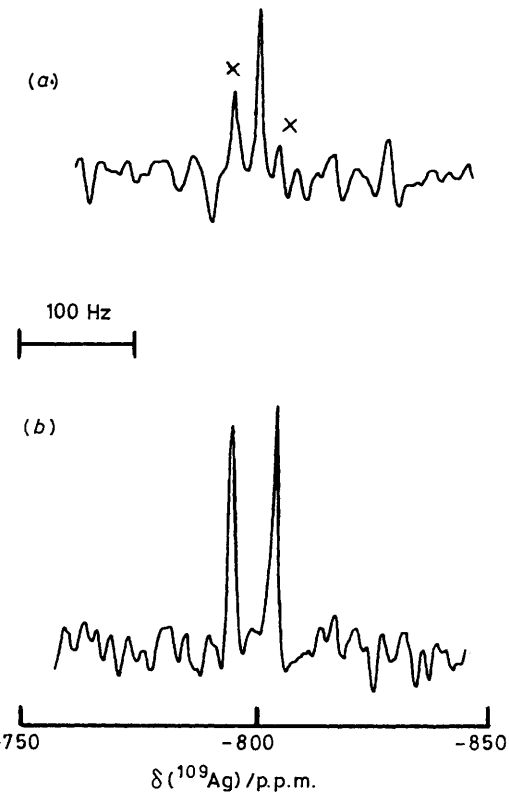

Figure 6. ^{109}Ag-{^{1}H} INEPT n.m.r. spectra of $[Ag_2Ru_4(\mu_3\text{-}H)_2(\mu\text{-}Ph_2AsCH_2AsPh_2)(CO)_{12}]$ (**7**), measured at 4.17-{89.6} MHz with proton decoupling during data acquisition. The spectra were recorded in CH_2Cl_2–C_6D_6 (*ca.* 4:1) solution at ambient temperature. (*a*) With the INEPT timings optimized to enhance the signals from the $^{109}Ag^{109}Ag$ isotopomer; (*b*) with the INEPT timings optimized to enhance the signals from the $^{107}Ag^{109}Ag$ isotopomer. In (*a*), the main peak is flanked by vestigial peaks due to the $^{107}Ag^{109}Ag$ isotopomer (marked ×)

* Similar dynamic behaviour, involving site-exchange of the arsenic and phosphorus atoms of a $Ph_2As(CH_2)_2PPh_2$ ligand between two cobalt atoms, would provide an alternative explanation for the rapid interconversion observed on the n.m.r. time-scale for the two enantiomers of $[Co_3(\mu_3\text{-}CCO_2CHMe_2)\{\mu\text{-}Ph_2As(CH_2)_2PPh_2\}(CO)_7]$ at ambient temperature in solution. Originally, a mechanism involving site-exchange of just the arsenic terminus of the bidentate ligand between two cobalt atoms, together with a concomitant carbonyl ligand migration and rotation of the $Co(CO)_2P$ vertex, was proposed to explain the racemization (K. A. Sutin, J. W. Kolis, M. Mlekuz, P. Bougeard, B. G. Sayer, M. A. Quilliam, R. Faggiani, C. J. L. Lock, M. J. McGlinchey, and G. Jaouen, *Organometallics*, 1987, **6**, 439). However, the alternative mechanism would also be expected to racemise the two enantiomers of the cluster $[Co_2Mo(\mu_3\text{-}CCO_2CHMe_2)\{\mu\text{-}Ph_2As(CH_2)_2PPh_2\}(CO)_6(\eta\text{-}C_5H_5)]$, in which the bidentate ligand bridges two cobalt atoms. As the above authors observed no such racemization for the mixed-metal species, their original mechanism seems more reasonable.

Table 4. Quantities of bidentate ligand used and product obtained and the chromatography conditions employed for the synthesis of the clusters $[M_2Ru_4(\mu_3\text{-}H)_2\{\mu\text{-}Ph_2As(CH_2)_nEPh_2\}(CO)_{12}]$ (M = Cu or Ag; E = As or P; n = 1 or 2)

		Quantity of $Ph_2As(CH_2)_nEPh_2$ used	Quantity of product obtained		Chromatography conditions *	
n	E		M = Cu	M = Ag	M = Cu	M = Ag
1	P	0.14 g, 0.33 mmol	0.32 g	0.31 g	Florisil	Alumina
2	P	0.15 g, 0.34 mmol	0.31 g	0.30 g	Florisil	Alumina
1	As	0.16 g, 0.34 mmol	0.27 g	0.35 g	Florisil	Florisil
2	As	0.16 g, 0.33 mmol	0.29 g	0.33 g	Florisil	Florisil

* Chromatography was performed on a 20 × 3 cm column at −20 °C, using a dichloromethane–light petroleum (1:1) mixture for elution.

dynamic behaviour. We chose to study (**7**), as the poor solubility of (**8**) in all common organic solvents did not allow sufficient sample to be dissolved to obtain a good quality spectrum. As for the analogous clusters containing $Ph_2P(CH_2)_nPPh_2$,[1] the special features of the spin systems in (**7**) allow the INEPT timings to be modified to produce spectra in which the signals due to either the $^{109}Ag^{109}Ag$ or the $^{107}Ag^{109}Ag$ isotopomer are predominant and those from the other species appear only as vestigial peaks (Figure 6). The spectra for (**7**) are much simpler than those previously reported for $[Ag_2Ru_4(\mu_3\text{-}H)_2\{\mu\text{-}Ph_2P(CH_2)_nPPh_2\}(CO)_{12}]$ (n = 1, 2, or 4),[1] as no second-order effects or ^{109}Ag–^{31}P and ^{31}P–^{31}P couplings occur for the former species. Only a single silver resonance is observed for each isotopomer, directly confirming that (**7**) exhibits dynamic behaviour involving silver atom site-exchange at ambient temperature in solution. The signal for the $^{109}Ag^{109}Ag$ isotopomer is a singlet, whereas that for the $^{107}Ag^{109}Ag$ isotopomer is split into a doublet by coupling to ^{107}Ag. The observed magnitude of $J(^{107}Ag^{109}Ag)$ is 40 Hz, which is similar to values obtained for the analogous clusters containing $Ph_2P(CH_2)_nPPh_2$ (35—42 Hz), but is 5 Hz larger than that reported for $[Ag_2Ru_4(\mu_3\text{-}H)_2(\mu\text{-}Ph_2PCH_2PPh_2)(CO)_{12}]$.[1]

The ^{109}Ag chemical shift of (**7**) is *ca.* 650 p.p.m. lower than that of the analogous cluster containing $Ph_2PCH_2PPh_2$.[1] This increase in shielding can probably be mainly attributed to the 'bulky substituent' effect of the more polarizable arsenic atoms. This effect is well established for the shielding of a non-transition element, for example tin,[13] and as the silver atoms in (**7**) have filled *d* shells, they must be regarded as 'non-transitional.' The metal shieldings may also be sensitive to changes in the interbond angles.

Experimental

All reactions and manipulations were performed under an atmosphere of dry oxygen-free nitrogen, using Schlenk-tube techniques.[14] Solvents were freshly distilled under nitrogen from the usual drying agents immediately before use. Light petroleum refers to that fraction of b.p. 40—60 °C. Established methods were used to prepare $[N(PPh_3)_2]_2[Ru_4(\mu\text{-}H)_2(CO)_{12}]$,[9] $[Cu(NCMe)_4]PF_6$,[15] and $Ph_2As(CH_2)_nPPh_2$ (n = 1[16] or 2[17]). The complex $[Ag(NCMe)_4]PF_6$ was synthesized by adaptation of a published route.[15] The ligands $Ph_2As(CH_2)_nAsPh_2$ (n = 1 or 2) were purchased from Strem Chemicals Inc. and used without further purification. Analytical and other physical data for the new compounds are presented in Table 1, together with their i.r. spectra. Table 2 summarizes the results of n.m.r. spectroscopic measurements.

Infrared spectra were recorded on a Perkin-Elmer 299B spectrophotometer. Hydrogen-1, $^{13}C\text{-}\{^1H\}$, and $^{31}P\text{-}\{^1H\}$ n.m.r. spectra were measured on Bruker AM 250 or WH 400 spectrometers. The $^{109}Ag\text{-}\{^1H\}$ INEPT n.m.r. spectra were recorded as previously described.[1] Product separation by column chromatography was performed on Aldrich Florisil (100—200 mesh) or B.D.H. alumina (Brockman activity II).

Synthesis of the Compounds $[M_2Ru_4(\mu_3\text{-}H)_2\{\mu\text{-}Ph_2As(CH_2)_nEPh_2\}(CO)_{12}]$ (M = Cu *or* Ag; E = As *or* P; n = 1 *or* 2).—A dichloromethane (40 cm^3) solution of $[N(PPh_3)_2]_2[Ru_4(\mu\text{-}H)_2(CO)_{12}]$ (0.60 g, 0.33 mmol) at −30 °C was treated with a solution of $[M(NCMe)_4]PF_6$ (M = Cu, 0.25 g, 0.67 mmol; M = Ag, 0.28 g, 0.67 mmol) in dichloromethane (30 cm^3) and then, after stirring the reaction mixture at −30 °C for 1 min, a dichloromethane (20 cm^3) solution containing the appropriate amount (Table 4) of the desired bidentate ligand $Ph_2As(CH_2)_nEPh_2$ was added. The mixture was allowed to warm to ambient temperature with stirring and the solvent was removed under reduced pressure. The residue was extracted with dichloromethane–diethyl ether (1:4, 50 cm^3 portions) until the extracts were no longer coloured red and the combined extracts were then filtered through a Celite pad (*ca.* 1 × 3 cm). After removal of the solvent under reduced pressure, the crude residue was dissolved in dichloromethane–light petroleum (1:1) and chromatographed under the appropriate conditions (Table 4). The chromatography afforded one red fraction in each case, which, after removal of the solvent under reduced pressure and crystallization of the residue from dichloromethane–light petroleum, yielded dark red *microcrystals* of $[M_2Ru_4(\mu_3\text{-}H)_2\{\mu\text{-}Ph_2As(CH_2)_nEPh_2\}(CO)_{12}]$. Table 4 lists the amounts of product obtained.

Crystal Structure Determination for (**2**).—Suitable crystals of (**2**) were grown from a diethyl ether–light petroleum mixture by slow layer diffusion at −20 °C.

Crystal data. $C_{38}H_{26}AsCu_2O_{12}PRu_4$, M = 1 311.88, monoclinic, space group $P2_1$, a = 12.614(3), b = 27.526(4), c = 13.888(2) Å, β = 105.46(2)°, U = 4 648(1) Å^3, Z = 4, D_c = 1.875 g cm^{-3}, $F(000)$ = 2 528, λ = 0.710 69 Å, μ(Mo-K_α) = 29.4 cm^{-1}, crystal size 0.63 × 0.28 × 0.10 mm.

Data collection. Unit-cell parameters and intensity data were obtained by following previously detailed procedures,[18] using a CAD4 diffractometer operating in the ω–2θ scan mode, with graphite-monochromated Mo-K_α radiation. A total of 8 346 unique reflections were collected ($3 \leqslant 2\theta \leqslant 50°$). The segment of reciprocal space scanned was: h −15—15, k 0—32, l 0—16. The reflection intensities were corrected for absorption, using the azimuthal-scan method;[19] maximum transmission factor 1.00, minimum value 0.86.

Structure solution and refinement. The structure was solved by the application of routine heavy-atom methods (SHELX 86[20]) and refined by full-matrix least-squares (SHELX 76[21]). The asymmetric unit contains two independent molecules, which are essentially chemically equivalent. However, from the refined values of the $U_{iso.}$ parameters for the two sets of As and P atoms, there would seem to be some mixing of As and P at each site. In each case, the sites are predominantly as labelled (Figure 2), which corresponds to isomer **B** (Figure 1), but there would seem to be more mixing in molecule 1 ($U_{iso.}$ for As 0.068; $U_{iso.}$ for P 0.011 Å^2) than in molecule 2 ($U_{iso.}$ for As 0.053; $U_{iso.}$ for P 0.028 Å^2). In view of the level of refinement possible for this large structure, which is dominated by heavy atoms, we did not consider it worthwhile to attempt to quantify these mixed occupancies.

Only the metal atoms, Ru and Cu, were refined anisotropically. Phenyl rings were refined as rigid groups (C–H 1.395 Å) and all hydrogen atoms were placed into calculated positions (C–H 0.96, Cu–H 1.62, Ru–H 1.80 Å; U = 0.10 Å^2).

Table 5. Atomic positional parameters (fractional co-ordinates) ($\times 10^4$) for $[Cu_2Ru_4(\mu_3\text{-}H)_2\{\mu\text{-}Ph_2As(CH_2)_2PPh_2\}(CO)_{12}]$ (**2**), with estimated standard deviations in parentheses

(*a*) Molecule 1

Atom	*x*	*y*	*z*
Ru(11)	3 640(2)	−1 999	−2 333(1)
Ru(12)	2 205(2)	−2 572(1)	−1 597(1)
Ru(13)	1 601(2)	−1 602(1)	−1 991(1)
Ru(14)	1 422(2)	−2 292(1)	−3 592(1)
Cu(11)	353(2)	−1 469(1)	−3 799(2)
Cu(12)	2 361(2)	−1 421(1)	−3 667(2)
As(11)	2 381(3)	−853(1)	−4 825(2)
P(11)	−655(3)	−850(2)	−4 658(3)
O(11)	5 265(23)	−1 364(11)	−2 978(20)
O(12)	4 845(17)	−2 907(9)	−2 569(15)
O(13)	4 877(19)	−1 907(9)	−146(17)
O(14)	3 265(20)	−3 568(10)	−1 670(17)
O(15)	3 186(19)	−2 506(10)	663(18)
O(16)	153(22)	−3 050(10)	−1 383(19)
O(17)	2 528(21)	−1 339(10)	189(19)
O(18)	986(18)	−527(9)	−2 369(15)
O(19)	−686(26)	−1 938(13)	−1 754(22)
O(110)	620(18)	−2 046(9)	−5 769(17)
O(111)	−797(20)	−2 672(9)	−3 576(17)
O(112)	2 172(19)	−3 280(9)	−4 116(16)
C(1)	302(18)	−384(9)	−5 012(17)
C(2)	979(19)	−592(9)	−5 570(17)
C(11)	4 594(25)	−1 597(12)	−2 778(21)
C(12)	4 330(23)	−2 583(11)	−2 456(20)
C(13)	4 399(20)	−1 951(10)	−1 015(17)
C(14)	2 812(22)	−3 166(11)	−1 675(19)
C(15)	2 800(24)	−2 534(12)	−168(22)
C(16)	929(25)	−2 859(12)	−1 442(21)
C(17)	2 155(23)	−1 463(11)	−618(20)
C(18)	1 204(20)	−946(10)	−2 299(17)
C(19)	226(28)	−1 822(13)	−1 826(24)
C(110)	951(21)	−2 100(10)	−4 956(19)
C(111)	91(22)	−2 548(10)	−3 532(18)
C(112)	1 897(22)	−2 898(11)	−3 872(19)
C(1A1)	−1 634(14)	−1 009(7)	−5 881(10)
C(1A2)	−1 866(14)	−696(7)	−6 700(10)
C(1A3)	−2 596(14)	−839(7)	−7 598(10)
C(1A4)	−3 094(14)	−1 295(7)	−7 677(10)
C(1A5)	−2 862(14)	−1 608(7)	−6 858(10)
C(1A6)	−2 132(14)	−1 465(7)	−5 960(10)
C(1B1)	−1 480(12)	−488(6)	−4 006(11)
C(1B2)	−1 179(12)	−24(6)	−3 629(11)
C(1B3)	−1 837(12)	227(6)	−3 132(11)
C(1B4)	−2 796(12)	13(6)	−3 011(11)
C(1B5)	−3 097(12)	−451(6)	−3 388(11)
C(1B6)	−2 439(12)	−702(6)	−3 885(11)
C(1C1)	3 038(14)	−1 048(7)	−5 843(11)
C(1C2)	2 419(14)	−1 325(7)	−6 636(11)
C(1C3)	2 912(14)	−1 517(7)	−7 340(11)
C(1C4)	4 023(14)	−1 431(7)	−7 252(11)
C(1C5)	4 642(14)	−1 154(7)	−6 460(11)
C(1C6)	4 150(14)	−962(7)	−5 755(11)
C(1D1)	3 112(13)	−289(6)	−4 323(11)
C(1D2)	3 259(13)	87(6)	−4 951(11)
C(1D3)	3 865(13)	497(6)	−4 549(11)
C(1D4)	4 323(13)	533(6)	−3 520(11)
C(1D5)	4 176(13)	158(6)	−2 893(11)
C(1D6)	3 571(13)	−253(6)	−3 294(11)

(*b*) Molecule 2

Atom	*x*	*y*	*z*
Ru(21)	137(2)	1 565(1)	8 682(1)
Ru(22)	1 777(2)	2 030(1)	8 014(1)
Ru(23)	2 130(2)	1 050(1)	8 491(1)
Ru(24)	2 348(1)	1 780(1)	10 033(1)
Cu(21)	3 245(2)	930(1)	10 388(2)
Cu(22)	1 216(2)	942(1)	10 067(2)
As(21)	1 072(2)	351(1)	11 184(2)
P(21)	4 178(4)	325(2)	11 260(3)
O(21)	−817(23)	2 563(11)	8 930(20)
O(22)	−926(23)	1 483(10)	6 407(21)
O(23)	−1 668(22)	1 064(10)	9 364(18)
O(24)	839(18)	3 053(9)	7 894(16)
O(25)	1 015(21)	1 958(10)	5 741(19)
O(26)	4 071(17)	2 388(8)	8 064(15)
O(27)	4 456(15)	1 283(7)	8 349(13)
O(28)	2 642(14)	−13(7)	8 981(12)
O(29)	1 321(17)	757(8)	6 270(15)
O(210)	4 777(16)	1 929(7)	10 233(14)
O(211)	2 123(19)	2 886(9)	10 265(16)
O(212)	2 656(19)	1 634(9)	12 281(17)
C(3)	3 222(19)	−123(9)	11 513(17)
C(4)	2 407(21)	70(10)	12 042(18)
C(21)	−428(24)	2 180(12)	8 809(21)
C(22)	−529(29)	1 632(14)	7 318(26)
C(23)	−931(24)	1 218(11)	9 134(20)
C(24)	1 285(23)	2 641(11)	8 003(19)
C(25)	1 368(20)	1 980(9)	6 622(17)
C(26)	3 205(21)	2 234(10)	8 049(18)
C(27)	3 576(20)	1 210(9)	8 428(17)
C(28)	2 380(20)	385(10)	8 899(17)
C(29)	1 640(22)	902(10)	7 141(19)
C(210)	3 786(19)	1 884(9)	10 136(16)
C(211)	2 106(23)	2 432(12)	10 117(20)
C(212)	2 478(23)	1 639(11)	11 331(20)
C(2A1)	5 073(14)	11(7)	10 598(13)
C(2A2)	4 935(14)	−474(7)	10 299(13)
C(2A3)	5 601(14)	−676(7)	9 746(13)
C(2A4)	6 404(14)	−393(7)	9 493(13)
C(2A5)	6 542(14)	92(7)	9 793(13)
C(2A6)	5 877(14)	294(7)	10 345(13)
C(2B1)	5 012(14)	430(7)	12 507(10)
C(2B2)	5 649(14)	61(7)	13 065(10)
C(2B3)	6 307(14)	158(7)	14 025(10)
C(2B4)	6 329(14)	623(7)	14 426(10)
C(2B5)	5 693(14)	992(7)	13 868(10)
C(2B6)	5 034(14)	896(7)	12 908(10)
C(2C1)	283(13)	−201(5)	10 595(11)
C(2C2)	−103(13)	−223(5)	9 556(11)
C(2C3)	−687(13)	−630(5)	9 102(11)
C(2C4)	−885(13)	−1 014(5)	9 686(11)
C(2C5)	−499(13)	−992(5)	10 724(11)
C(2C6)	85(13)	−585(5)	11 178(11)
C(2D1)	352(16)	544(8)	12 193(13)
C(2D2)	−759(16)	434(8)	12 051(13)
C(2D3)	−1 296(16)	573(8)	12 765(13)
C(2D4)	−722(16)	822(8)	13 620(13)
C(2D5)	388(16)	932(8)	13 762(13)
C(2D6)	926(16)	793(8)	13 048(13)

The final residuals R and R' were 0.059 and 0.064, respectively, for the 440 variables and 5 924 data for which $F_o > 6\sigma(F_o)$. The absolute configuration of the structure was tested (SHELX 76,[21] $R = 0.064$). The function minimized was $\Sigma w(|F_o| - |F_c|)^2$ with the weight, w, being defined as $1/[\sigma^2(F_o) + 0.001F_o^2]$.

Atomic scattering factors and anomalous scattering parameters were taken from refs. 22 and 23, respectively. All computations were performed on a DEC VAX-11/750 computer. Table 5 lists the atomic co-ordinates for the non-hydrogen atoms and selected bond lengths and angles are given in Table 3. Additional material available from the Cambridge

Crystallographic Data Centre comprises H-atom co-ordinates, thermal parameters, and remaining bond lengths and angles.

Acknowledgements

We thank Drs. O. W. Howarth and E. Curzon for recording a number of 400-MHz ^{1}H n.m.r. spectra, the S.E.R.C. for a studentship (to S. S. D. B.) and an allocation of time on their *X*-ray crystallographic service at Queen Mary College, the Nuffield Foundation for support, Johnson Matthey Ltd. for a generous loan of silver and ruthenium salts, Mr. R. J. Lovell for technical assistance, and Mrs. L. J. Salter for drawing the diagrams.

References

1 Part 9, S. S. D. Brown, I. D. Salter, V. Šik, I. J. Colquhoun, W. McFarlane, P. A. Bates, M. B. Hursthouse, and M. Murray, *J. Chem. Soc., Dalton Trans.*, 1988, 2177.
2 See, for example, M. J. Freeman, A. G. Orpen, and I. D. Salter, *J. Chem. Soc., Dalton Trans.*, 1987, 1001 and refs. therein.
3 C. E. Briant, K. P. Hall, and D. M. P. Mingos, *J. Chem. Soc., Chem. Commun.*, 1983, 843; J. A. K. Howard, I. D. Salter, and F. G. A. Stone, *Polyhedron*, 1984, **3**, 567; S. R. Bunkhall, H. D. Holden, B. F. G. Johnson, J. Lewis, G. N. Pain, P. R. Raithby, and M. J. Taylor, *J. Chem. Soc., Chem. Commun.*, 1984, 25.
4 S. S. D. Brown, S. Hudson, I. D. Salter, and M. McPartlin, *J. Chem. Soc., Dalton Trans.*, 1987, 1967.
5 T. Adatia, M. McPartlin, and I. D. Salter, *J. Chem. Soc., Dalton Trans.*, 1988, 751.
6 S. S. D. Brown, I. D. Salter, and L. Toupet, *J. Chem. Soc., Dalton Trans.*, 1988, 757.
7 S. S. D. Brown, I. D. Salter, D. B. Dyson, R. V. Parish, P. A. Bates, and M. B. Hursthouse, *J. Chem. Soc., Dalton Trans.*, 1988, 1795.
8 S. S. D. Brown, P. J. McCarthy, and I. D. Salter, *J. Organomet. Chem.*, 1986, **306**, C27.
9 S. S. D. Brown and I. D. Salter, *Organomet. Synth.*, in the press.
10 M. J. Freeman, A. G. Orpen, and I. D. Salter, *J. Chem. Soc., Dalton Trans.*, 1987, 379.
11 P. A. Bates, S. S. D. Brown, A. J. Dent, M. B. Hursthouse, G. F. M. Kitchen, A. G. Orpen, I. D. Salter, and V. Šik, *J. Chem. Soc., Chem. Commun.*, 1986, 600.
12 R. A. Brice, S. C. Pearse, I. D. Salter, and K. Henrick, *J. Chem. Soc., Dalton Trans.*, 1986, 2181.
13 J. D. Kennedy and W. McFarlane, in 'Multinuclear N.M.R.,' ed. J. Mason, Plenum Press, London and New York, 1987, p. 305; A. G. Davies, P. G. Harrison, J. D. Kennedy, T. N. Mitchell, R. J. Puddephatt, and W. McFarlane, *J. Chem. Soc. C*, 1969, 1136.
14 D. F. Shriver, 'The Manipulation of Air-Sensitive Compounds,' McGraw-Hill, New York, 1969.
15 G. J. Kubas, *Inorg. Synth.*, 1979, **19**, 90.
16 R. Appel, K. Geisler, and H-F. Schöler, *Chem. Ber.*, 1979, **112**, 648.
17 W. Levason and C. A. McAuliffe, *Inorg. Synth.*, 1976, **16**, 191.
18 M. B. Hursthouse, R. A. Jones, K. M. A. Malik, and G. Wilkinson, *J. Am. Chem. Soc.*, 1979, **101**, 4128.
19 A. C. T. North, D. C. Phillips, and F. S. Mathews, *Acta Crystallogr., Sect. A*, 1968, **24**, 351.
20 G. M. Sheldrick, SHELX 86, Program for Crystal Structure Solution, University of Göttingen, 1986.
21 G. M. Sheldrick, SHELX 76, Program for Crystal Structure Determination and Refinement, University of Cambridge, 1976.
22 D. T. Cromer and J. B. Mann, *Acta Crystallogr., Sect. A*, 1968, **24**, 321.
23 D. T. Cromer and D. Liberman, *J. Chem. Phys.*, 1970, **53**, 1891.

Received 9th December 1987; *Paper* 7/2162